Time-gated real-time bioimaging system using multicolor microsecond-lifetime silica nanoparticles

Dayong Jin[1*], James Piper[1], Jingli Yuan[2], Robert Leif[3],

[1]MQ Photonics Centre, Faculty of Science, Macquarie University, NSW 2109, Sydney, Australia

[2]State Key Laboratory of Fine Chemicals, Dalian University of Technology, Dalian 116012, P. R. China

[3]Newport Instruments, 5648 Toyon Road, San Diego, CA, USA 92115-1022

ABSTRACT

In advanced cytometry, a fundamental challenge for rapid specific detection of rare-event micro-organisms is the autofluorescence noise from the complex biological samples. Time-gated luminescence can effectively discriminate labeled cells from autofluorescence background. Recently, a real-time true-colour time-gated luminescence microscopy system has been developed based on the synchronization of a solid-state excitation source and a super-fast optical shutter. We also developed a variety of ultra-bright silica nano-biolabels with multiple luminescence colours and controllable lifetimes in microsecond range. These developments allowed the development of an advanced cell analysis system for real-time background-free imaging and rare-event counting of microsecond-lifetime multi-colour labelled water-borne pathogens.

Key words: time-gated luminescence, real-time imaging, silica nanoparticle, europium, terbium, lanthanide, waterborne, pathogen, microscopy, lifetime, autofluorescence

INTRODUCTION

Recent decades have witnessed many important advances in fluorescence microscopy for cellular imaging including confocal fluorescence microscopy and multi-photon fluorescence microscopy. These cellular imaging techniques are often associated with specific fluorescence biolabels— from organic dyes to fluorescent proteins and semiconductor quantum dots. Usually they are sensitive enough to explore even sub-cellular information, however, since the majority of these techniques are based on spatial variation of emission intensity or on wavelength band differences, when applying to, for example, rare-event detection (1 target event in > 10^5 non-target background microorganisms) [1,2], immunocytochemistry or in situ nucleic acid hybridization intracellular assays [3], these fluorescence microscopes suffer from two drawbacks affecting measurement sensitivities: the autofluorescence from non-target bio-samples (spectral overlapping) and light scattering from nearby optics.

Since the first lanthanide based imaging was suggested in 1976 [4] and the first bioassays implemented for immunodiagnostics in 1983 [5], luminescent lanthanide bioprobes have become one of the most sensitive luminescence probes in clinical diagnostics and bioanalytical chemistry[6,7]. Thanks to several distinct advantages, including exceptional-long lifetime (micro-to-milliseconds), large Stokes shift (typically ~ 200 nm) and sharp emission profile (~ 10 nm width at half maximum), an absence of concentration quenching,

* send all correspondence to: Dr. Dayong Jin, jin@science.mq.edu.au, phone 61 2 9850 4168, Fax: +61-2-98508115

Imaging, Manipulation, and Analysis of Biomolecules, Cells, and Tissues VIII, edited by Daniel L. Farkas, Dan V. Nicolau, Robert C. Leif, Proc. of SPIE Vol. 7568, 756819 · © 2010 SPIE · CCC code: 1605-7422/10/$18 · doi: 10.1117/12.841569

and distance-dependent luminescence resonance energy transfer (LRET) properties (with larger measurable distance range >100 Å and significantly greater accuracy[8]), this new class of labels offers the potential of simultaneous temporal-spectral-spatial 3-Dimentional discrimination power for ultra-high-contrast biosensing applications [6,9] including immunoassay, DNA assay, high-contrast microscopy bioimaging and rare-event flow cytometry [2]. Recent developments of highly fluorescence lanthanide complexes [3,10,11], responsive lanthanide-based luminescent probes [12], functionalized lanthanide Ions nanocomposites [13], and nano-encapsulation lanthanide containing biolabels [14-16] have particularly promoted the importance of lanthanide based cellular imaging applications. However, the weak slowly cycling luminescence (in principle a fluorophore is capable of being excited once for roughly each lifetime, τ in order of $>10^4$ of conventional biolabels [17]) in nature requires usually more than 30-second signal accumulation in order to produce a quality time-gated luminescence (TGL) image, thus researchers reported either grayscale[18,19] or pseudocolor [9,14,20] TGL cell images by high-quality monochrome (high-gain) cameras. Though the impressive suppression of background autofluorescence was demonstrated in time domain by taking the advantage of large degree difference in lifetime (ns versus μs), the important spectrum information was traded off. To our best knowledge, none of these developments and biological imaging applications is sufficiently bright to permit naked-eye direct observation with true-color TGL images (equivalently requiring as short as 1 second exposure time). The practical utilization of lanthanide luminescence by many of the current medical practioners requires that background-free lanthanide stained cells be observable directly by human eyes in real-time.

In this work, we applied both biolabel strategy (using nano-encapsulation technique for signal amplification) and optics strategy (using a new complimentary optics layout to design the time-gated luminescence microscopy) to increase the signal time-gated luminescence intensity, resulting in a new bioimaging system allowing direct observation of lanthanide stained cells by naked eyes at background-free condition.

MATERIALS AND METHODS

Nano-encapsulation technique & lanthanide containing silica nanoparticles

A reverse microemulsion is an isotropic and thermodynamically stable single-phase system consisting of water, oil and surfactant[21], (the cyclohexane and n-octanol as oil, triton X-100 as surfactant in our work, as shown in Figure 1). By appropriate stirring, the nanosized-droplets of water surrounded by surfactant are generated and dispersed in the continuous bulk oil phase. The nanosized water core will serve as confined nanomedia for the formation of discrete nanoparticles. The size of the end-product silica nanoparticles is typically determined by the size of the nanodroplet water core, which is controlled by the water-to-surfactant molar ratio (*W0*). The particle size was found to decrease with an increase in the concentration of ammonium hydroxide and with an increase in the water-to-surfactant molar ratio (*W0*) or the cosurfactant-to-surfactant molar ratio. The uniform micro-emulsion consisting of the nano-sized water droplets can be formed by 1 hour vigorous stirring. Instead of the direct dye-doping method, we developed a covalent binding-copolymerization method to prepare silica-based lanthanide nanoparticles [6,16]. In this method, a conjugate of (3-aminopropyl)triethoxysilane (APS) bound to a lanthanide complex was first prepared as precursor, so that the lanthanide complex dye can be firmly (covalently) bound to silicon atoms when forming silica nanoparticles through ammonia-catalyzed hydrolysis of tetraethylorthosilicate (TEOS) in those water-in-oil microemulsions. There are two advantages comparing to the dye-doping method, firstly the dye leaking problem in bioassay processes using the luminophore-doped nanoparticle probes can be effectively resolved. which permits the use of smaller particles. This decrease in size should increase the probability that these

small particles can enter a cell and thus be used to stain intracellular macromolecules. Furthermore, since the nanoparticles were prepared by copolymerization of APS-metal complex, free APS, and TEOS, free amino groups were directly introduced to the surface of the nanoparticles, and these amino groups made the surface modification and bioconjugation of the nanoparticles easier.

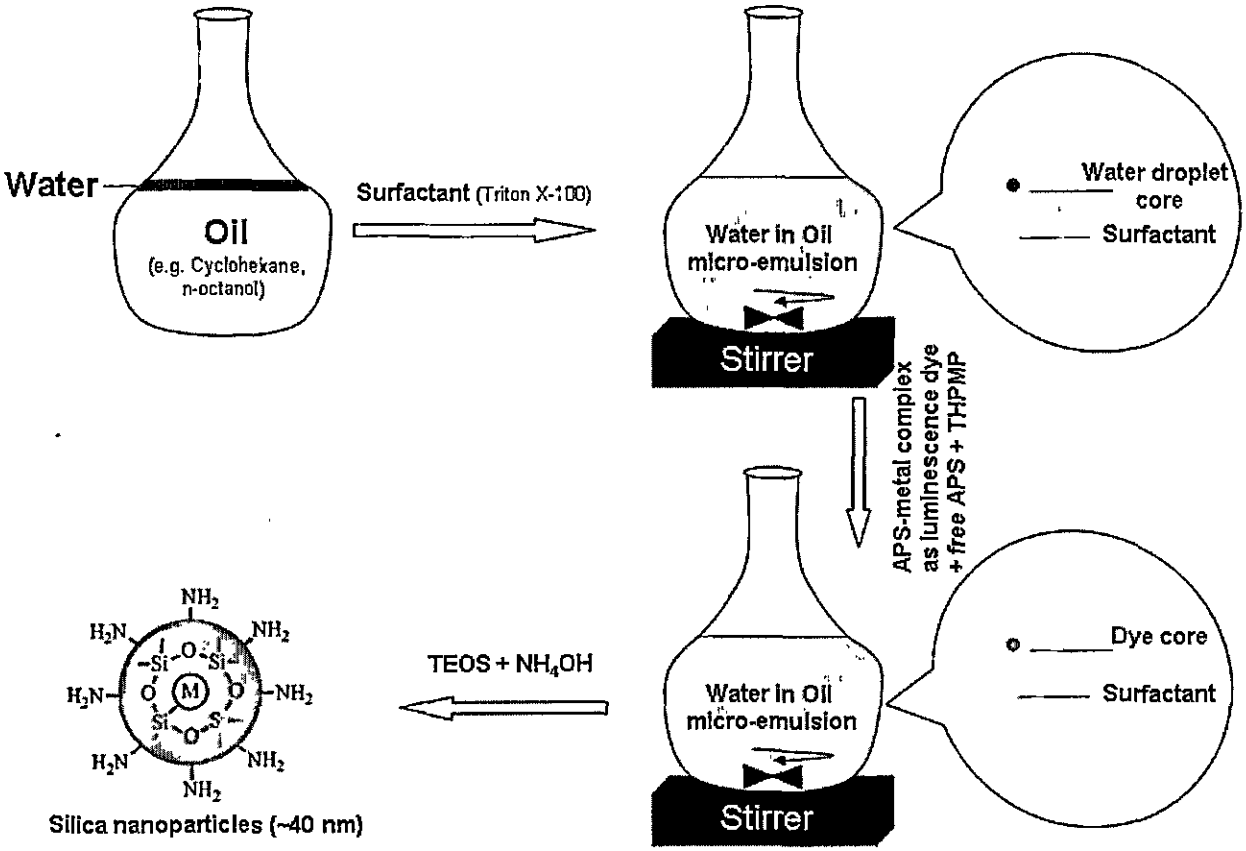

Figure 1. Schematics of covalent binding nano-encapsulation method to synthesize silica-based highly luminescent nanoparticles containing > 1,000 lanthanide metal complex

Preparation of multicolor luminescent lanthanide nanoparticles

The multi-color time-resolved fluorescence bioassays based on microsecond lifetime lanthanide compounds have been rarely investigated, because there are only Eu^{3+} (red 615 ± 10 nm) and Tb^{3+} (green, 545 ± 10 nm) compounds emitting strong fluorescence. We succeeded in synthesizing a series of silica nanoparticle biolabels emitting green, yellow, orange and red colors with an excitation peak at 335 nm. The new biolabels have been prepared by co-binding different molar ratios of fluorescent Eu^{3+}-Tb^{3+} complexes with a ligand N,N,N^1,N^1-(4'-phenyl-2,2':6',2"-terpyridine-6,6"-diyl) bis(methylenenitrilo) tetrakis (acetic acid) (PTTA) inside the silica nanoparticles.

In details, to a solution of 4.6 mg 1-ethyl-3-(3-dimethylaminopropyl) carbodiimide) (EDC) and 0.8 mg N-hydroxysuccinimide (NHS) dissolved in 80 µL of anhydrous ethanol was added a solution of 1.88 mg PTTA·1.5H_2O dissolved in 20 µL of 0.05 M sodium carbonate buffer of pH 9.5. The solution was stirred for 1

h at room temperature, and then 1.5 μL of APS was added. The reaction was continued for another 2 h, and then a 100 μL solution containing $EuCl_3/TbCl_3$ (total metal ion concentration is 0.03 M, molar ratio of Eu^{3+}/Tb^{3+} was 0:1, 1:5, 1:3, 1:1, 3:1, 5:1 and 1:0, respectively) was added to form the fluorescent precursor (APS-PTTA-Ln^{3+} conjugate, Ln = Eu or Tb).

To a water-in-oil (W/O) microemulsion prepared by mixing 1.77 g of Triton X-100, 5.8 g of cyclohexane, 1.32 g of 1-octanol, 1.5 μL of free APS and 300 μL of water was added the above precursor with stirring to make a homogenous solution. After the solution was stirred for 30 min at room temperature, 100 μL of TEOS and 60 μL of concentrated aqueous ammonia (25-28%) were added, and the reaction was allowed to continue for 24 h at room temperature. The final nanoparticles were isolated from the microemulsion by adding 20 mL of acetone, centrifuging, and washing with ethanol and water several times to remove the surfactant and unreacted materials. [This work reporting multi-color lanthanide silica nanoparticles has been recently accepted for publication by Journal of Fluorescence (DOI 10.1007/s10895-009-0559-7).]

Surface modification to make biocompatible nanoparticles

Carboxyl groups and PEG modification: Three milligrams of polyethylene glycol (NH2-PEG-COOH) (5,000MW) and 300μl of 1% glutaraldehyde were added to the 500microl of NPs solution with stirring for 22 hours at room temperature, the nanoparticle surface could easily be functioned with carboxyl groups. The PEGylated surface is highly hydrophilic and enhances the aqueous dispersion of the silica nanoparticles.

Straptiavidin and BSA: Due to the presence of surface amino groups, the nanoparticles can be directly conjugated to streptavidin (SA) molecules. To improve the low SA bio-activity on the nanoparticles, we established a BSA (bovine serum albumin) coating method to prepare the nanoparticle-labeled SA. The BSA-coated nanoparticles were then used for binding to SA by coupling the amino groups of BSA and SA with glutaraldehyde. For details, refer to our earlier publications[14,15]

Pathogen labeling

We use indirect immunofluorescence labeling by mouse monoclonal anti-Giardia IgG antibody G203 and Goat Anti-Mouse Light Chain Specific Biotin conjugated IgG antibody, for *Giardia Lamblia cysts*, and mouse monoclonal anti- *Cryptosporidium parvum* IgG antibody C104 and Goat Anti-Mouse Light Chain Specific Biotin Conjugated IgG antibody for *Cryptosporidium parvum oocysts*.

Cell uptake experiment

The mouse LAF1 pituitary gland tumor cells, AtT20, are cultured in Dulbecco's modified Eagles Medium supplemented with 10% fetal bovine serum. The day before experiment, the cells are split into a 4-well slide. And the cells are incubated with the nanoparticle solution diluted in 300 μL phosphate buffered saline for 60 min.

Time-gated Luminescence Microscopy (TGLM)

Applying a TGL sequence, consisting of a pulsed excitation, an appropriate time delay and time-gated detection, the short-lived background autofluorescence from the raw biological samples or scattering from nearby optics can be effectively eliminated (see Figure 2). Following a number of advanced developments of lanthanide based TGL microscopy in the recent decade[18,22], a comprehensive review of progress on TGL microscopy instrumentation development was recently published from this group[23]. The trend for pulsed excitation is moving from chopper interrupted CW Hg lamp or UV lasers to Xenon flashlamps to the recent UV LED excitation, while the trend for time-gated detection is shifting from chopper or ferro-electric shutter gated CCD to gated intensifier CCD and the recent electron-multiplying CCD [23]. We anticipate the factors limiting real-time naked-eye observation of lanthanide cellular staining can be attributed to the low "Average

TGL Signal Intensity" (defined as "accumulated time-gated luminescence over 1 second" in this work) collected by the previous TGL microscopes, which requires either/both long exposure time or/and high photo-electron gains from intensified CCD cameras or EMCCDs [18].

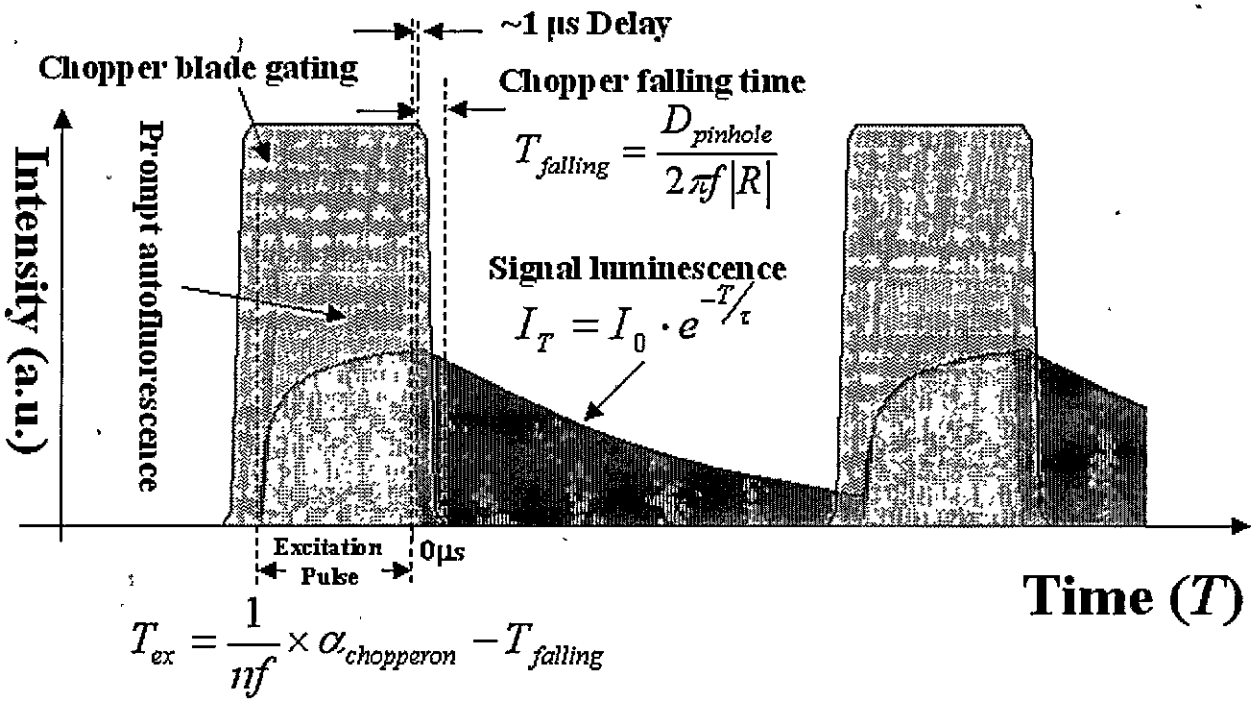

Figure 2. The Schematics of chopper gated long-lived luminescence bioimaging. $D_{pinhole}$, is the pinhole diameter, R, is the effective chopper blade radius, and f, is the chopper spinning frequency, n, is the chopper blade slots number, and $\alpha_{chopperon}$, is the blade blocking duty ratio. The higher time-gated luminescence cycle (consisting of pulsed excitation, appropriate time delay and gated detection) rate can increase the averaged TGL signal intensity over the observation period. A faster chopping switching time, $T_{falling}$, can contribute higher time-gated signal collection efficiency, permit longer excitation pulses T_{ex} and higher time-gated detection cycle frequency, nf, which will all together increase the average TGL signal intensity opening up new opportunities in naked eye direct observation or true-color CCD recording.

Figure 2 shows the principle of time-gated luminescence detection. The targets of interest are labeled with a long-lived luminescent probe, typically a lanthanide complex with luminescence lifetime > 100 μs. The autofluorescence fades rapidly (within 0.1 μs) following the switch-off of pulsed (75 μs UV LED pulse in this case) excitation, when the chopper blade completely blocks the optical path to detection. After the background autofluorescence ceases, the chopper blade is switched onto transparent phase, so that the majority signal luminescence can be detected at background-free condition. The following analysis shows important implications for optimum conditions in aspects of both excitation and signal collection:

1. Increasing TGL repetition rate will significantly increase the "Average TGL Signal Intensity", so that the best repetition rate for the luminescence lanthanide bioprobes should be in the range of 1 kHz to 10 kHz. This excludes most Xenon flash lamps (typically <100 Hz) and Nitrogen lasers (337 nm,

typically ~ 40 Hz). Nowadays UV LEDs or Diode-pumped Q-switched UV solid-state lasers (1 kHz to several MHz) are among the best choices.

2. For naked eye observation of time-gated luminescence, physical interrupting the emission pathway to eyes is essential. Either a ferro-electric shutter or a mechanical chopper should be used. For most lanthanide cell imaging applications, the collected emission is likely to be rotationally depolarised in solution[20], ferro-electric shutter suffers from typically up to 85% signal loss [23] and slow switching-on time (~80 μs). Still the mechanical chopper is simpler to install and low cost; however, previously reported time-gated luminescence microscopes[9,20,23,24] employing mechanical chopper require typically 100 μs to 200 μs switch-on time. Now the question is whether a faster switching-on time can be engineered.
3. As shown in Figure 2, once the TGL repetition rate (TGL period) is fixed, in order to increase the "Average TGL Signal Intensity", both excitation efficiency and TGL signal collection efficiency determine the TGL intensity in a single cycle. The excitation efficiency is function of chopper-on gating period and switching-on time, a faster switching-on time allows longer excitation pulse thus higher excitation efficiency (before the LED pulse reaches saturating power). The efficiency of single TGL cycle signal collection is determined by the portion of chopper blocked TGL light during the open-switching time, and a faster gating time results in less TGL signal loss. It can be concluded that faster switching-on time benefits both higher excitation efficiency and signal collection efficiency. The way to maximize the switching on time is either through using larger diameter chopper blade (higher linear speed) or chopping smaller beam diameter, or using faster spinning speed (however, the maximum spinning speed is typically related to the spin power and the physical characteristics of chopper blade).
4. The methods to reduce the chopper interrupted beam diameter is either through reduction of observation window area or spatially filtering the image plan by a smaller gating pinhole where the light travels through (see figure 3). $T_{falling} = \frac{D_{pinhole}}{|v|} = \frac{D_{pinhole}}{2\pi f |r|}$
5. One of the simple ideas is to bring the image to a focus by the eyepiece of the conventional fluorescence microscope, and to image the small focused image after it has been chopped image by second eyepiece onto the naked eye or digital camera, so that the new system functions without any complicated change of emission pathway. Alternatively, confocal epi-fluorescence optics can be employed with the chopper interrupting the confocal point.

In the prototype TGL microscope, we choose the most cost effective commercially available optical chopper (C995 Optical Chopper, Terahertz Technologies, Inc., NY) with maximum rotation rates of up to 167 RPS with effective chopper blade diameter r of 42 mm (the actual diameter of ~48 mm). We employed a pinhole (1.1 mm in diameter) behind the chopped (chopper interrupted) image plan, by adjusting the pinhole size and balance the spatial observation window, we achieved chopper falling speed as fast as 16 μs, which resulted in a observation window of ~ 450 μm in diameter on the specimen slide using ×20 objective. In practice, the ×60 objective or higher power objective used results in as fast switch-on time as 11 μs with ~ 160 μm in diameter observation window. In our prototype microscope, the LED (maximum CW output power of 250 mW at 365 nm, NCCU033A; Nichia Corp. Japan) excitation duration was 75 μs, and the repetition rate of 2500 Hz with duty ratio of 25%: 75%.

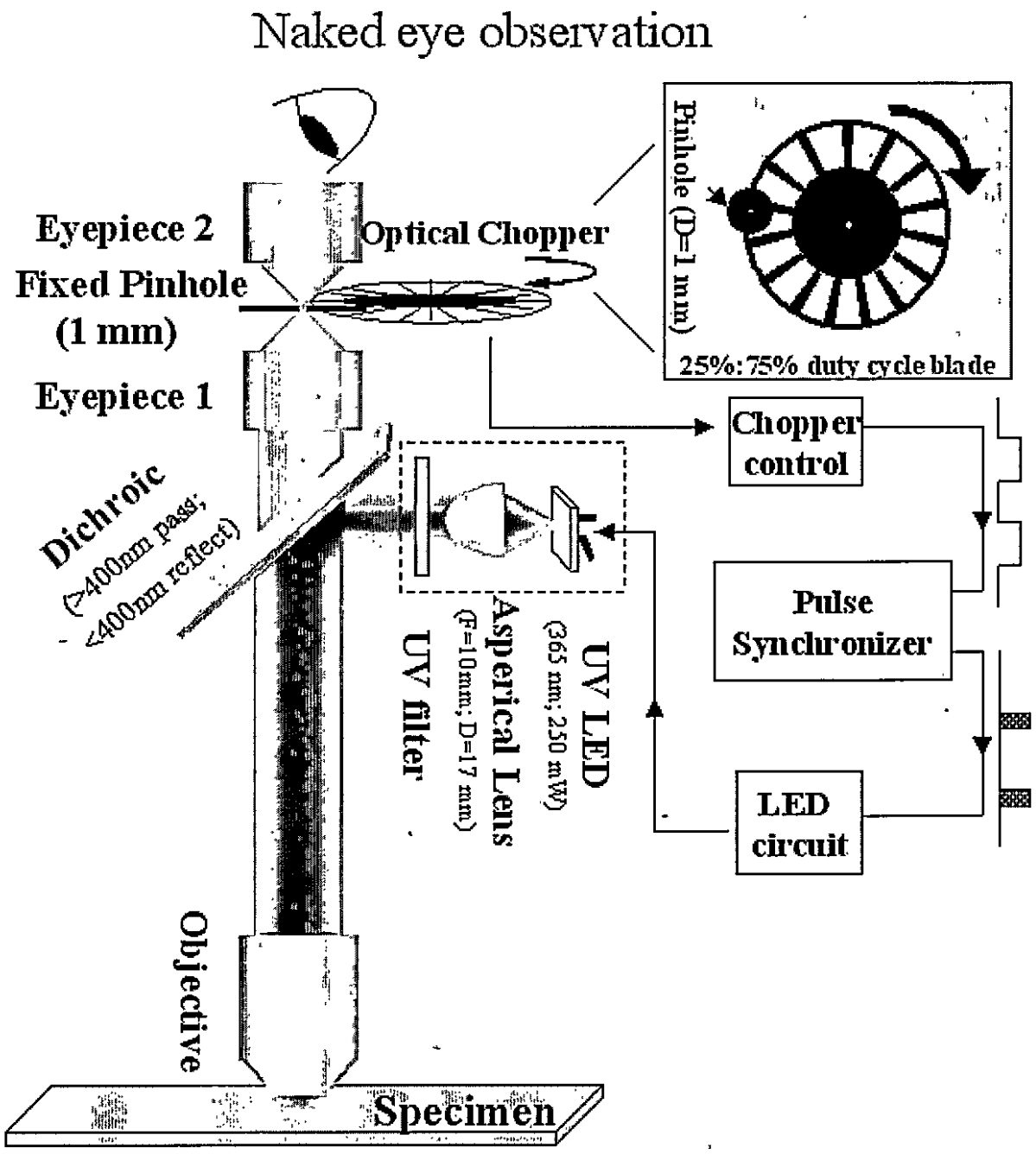

Figure 3. Schematic geometric layout of time-gated luminescence microscope: a method by chopper gating the imaging plan to achieve much faster chopper switching time and additional eyepiece to allow direct observation of time-gated luminescence. The pulse synchronizer accepting monitored TTL signal from chopper blade, was used to trigger the UV LED circuit, so that an appropriate time-delay between excitation pulse to gated-detection phase was achieved[25].

RESULTS

Silica nanoparticles

Figure 4A shows the TEM image of these uniform spherical nanoparticles in size ~ 40 nm, having fine monodispersity in aqueous solutions. Figure4B shows multi-color silica nanoparticles containing different ratio of europium: terbium. Characterizations by transmission electron microscopy (TEM) and fluorometric methods indicate that the nanoparticles are spherical and uniform in size with long fluorescence lifetimes (>1.0 ms) and high photostabilities.

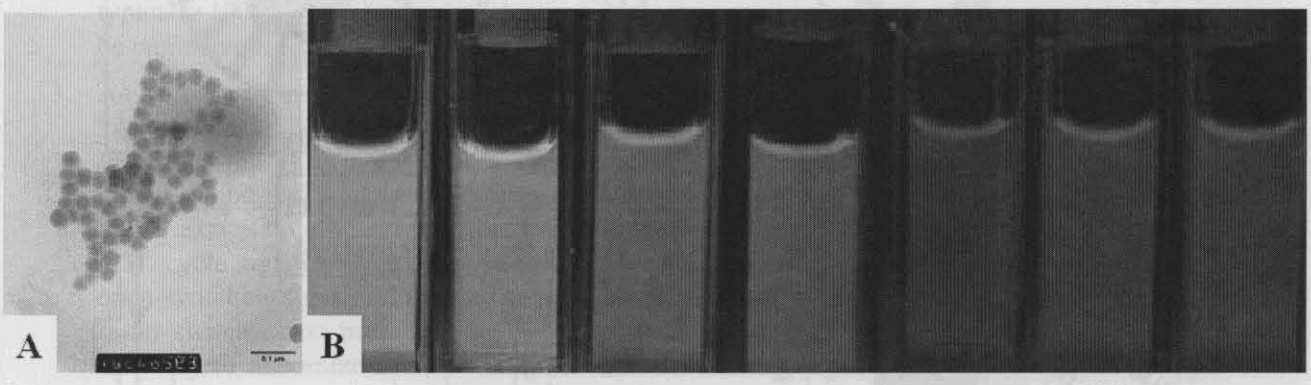

Figure 4. A). TEM image of these long-lifetime luminescence silica nanoparticles (the scale bar is 0.1 μm); B) Emission color images of the nanoparticles prepared with different molar ratios of PTTA-Eu^{3+}/PTTA-Tb^{3+} complexes in aqueous solution under irradiation of a 365 nm UV lamp (from left to right, Eu^{3+}:Tb^{3+} = 0:1, 1:5, 1:3, 1:1, 3:1, 5:1, 1:0)

Real-time inspection of pathogens

The new nanoparticles were successfully applied to distinguish two environmental pathogens, *Giardia lamblia* (shown in Figure 3), and *Cryptosporidium parvum oocysts* (shown in Figure 4) within a concentrate of environmental water sample using a time-gated luminescence microscope with pulsed UV LED excitation.

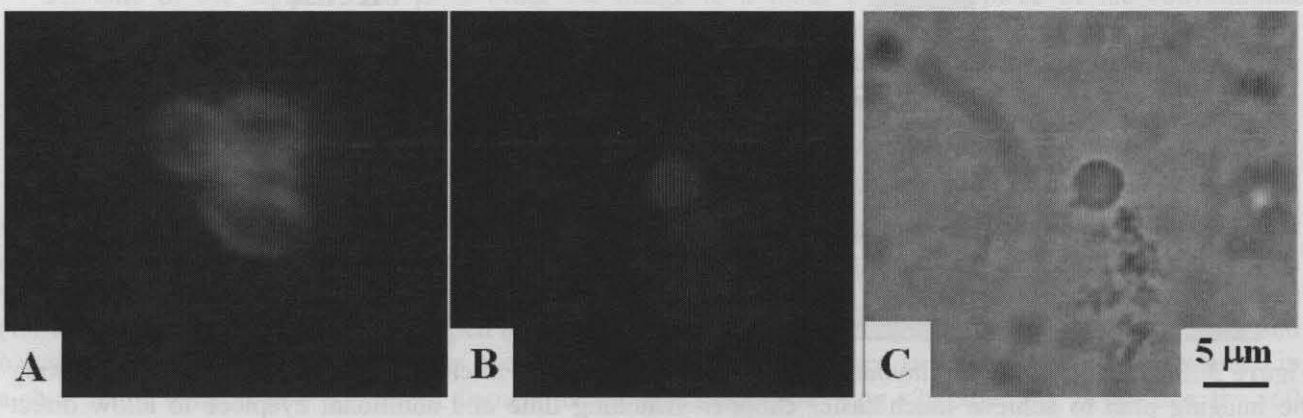

Figure 5 direct observations of environmental pathogen microorganisms by the new time-gated luminescence microscope. A), the europium silica nanoparticles labeled "3 *Giardia Lamblia cysts*"; B) and C), time-gated luminescence image (visible) and bright field image of the europium silica nanoparticles labeled "*Cryptosporidium oocyst*"

Cell uptake imaging at background-free condition

Also this new silica nanoparticles were successfully applied to cell uptake by the mouse LAF1 pituitary gland tumor cells. The time-gated luminescence microscopy technique results demonstrated in Figure 6 that the long-lived luminescence achieved background-free detection at intracellular levels. In particular demonstrated that the signal-to-background contrast is adjustable respecting to different application circumstances by different chopper speed settings.

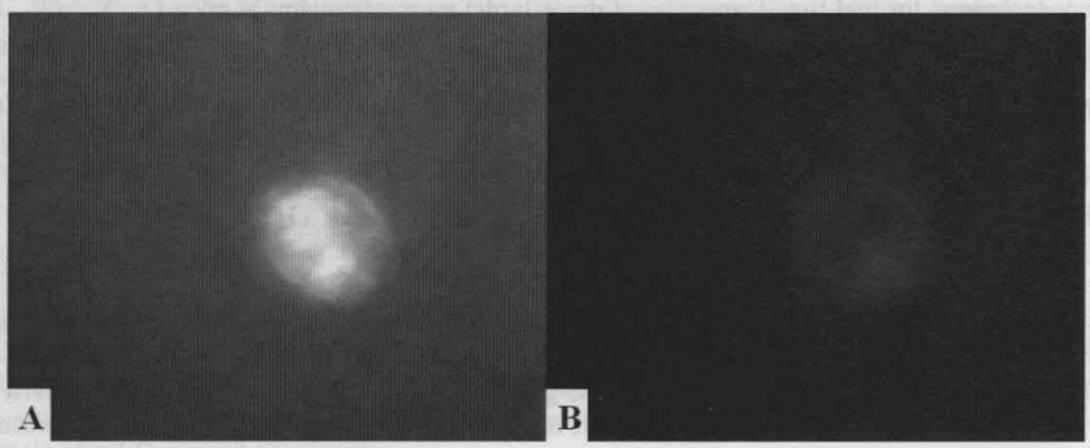

Figure 6 time-gated luminescence microscopy measurement of long-lifetime silica nanoparticle cell uptake (2.5 second exposure time by the Thorlabs USB2.0 CMOS industry camera (the camera only costs $200). A) conventional flourescence microscopy mode; B) virtually complete rejection of background (the signal-to-background contrast is adjustable by different chopper speed settings)

DISCUSSION AND CONCLUSION

By co-binding different molar ratios of fluorescent Eu^{3+}/Tb^{3+} complexes inside silica nanoparticles, a series of fluorescent lanthanide nanoparticles with multi-fluorescence colors has been prepared. The unique fluorescence properties of these nano-biolabels offer an opportunity for developing fluorescent multicolor biolabeling-based time-resolved fluorescence bioassay techniques, such as multi-label immunological, DNA hybridization and biochip assays.

Previous works [26] in time-gated luminescence bioimaging have resulted in high-contrast imaging by time-domain gating, however, due to the long signal integration time (typically > 30 seconds) required, the true color spectrum resolution was sacrificed due to the required gating using the sensitive monochrome cameras. The companion paper[27] in this volume describes an alternative approach; however, it has the present limitation of not permitting direct viewing by eye. In contrast with previous work, the new technique we developed in this work has proved successful for direct observation of time-gated lanthanide luminescence at background-free condition. The improved time-gated technique allows ultra-high contrast bioimaging through temporal, spectral, morphological and intensity resolutions, which render this unique time-gated luminescence imaging microscopy superior to the existing advanced microscopy techniques in many aspects, since the vast majority of fluorescence imaging studies to date has been based on spatial variation of emission intensity or on wavelength changes. Moreover, this technique can be easily applied to the common conventional fluorescence microscopes at very additional low-cost (<$2,000) and very limited engineering processes. One can simply gate the image plan behind the eyepiece by an optical chopper, and re-project the interrupted image by a second eyepiece behind, to realize direct observation of time-gated luminescence signals. We vision this practical technique potentially has a large impact on lanthanide (as well as phosphorescence dyes) based advanced biosensing areas, for example, continuous monitoring of biological cellular processes (e.g. celluar chemical sensing of pH, cations using lanthanide complexes as excellent sensors/switches) in real time

[12,28], tissue imaging (time-resolved)[29], and lanthanide sensitized FRET emission mapping (in which a long-lived chelate is used as energy transfer donor and a fluorophore with a lifetime in the nanosecond range as the acceptor[20]), as well as lifetime mapping[30]. Since the new microscope realized true-color imaging, the muliti-color lanthanide based time-gated luminescence imaging is also feasible[10].

With these newly developed multi-color nanoparticle biolabels, and true-color time-gated luminescence imaging cytometry, our next target is to explore the multiplexing detection opportunities using time-gated luminescence technique for real-time inspection of many target microorganisms at once.

Acknowledgements

The authors wish to acknowledge Australian Research Council (Discovery Project DP 1095465), Macquarie University Research Fellowship Scheme, the ISAC (International Society for Analytical Cytology) scholar program, the National Natural Science Foundation of China (No. 20575069), and Newport Instruments' Internal Development Funds.

References

[1] S. Bajaj, J. B. Welsh, R. C. Leif et al., "Ultra-rare-event detection performance of a custom scanning cytometer on a model preparation of fetal nRBCs," Cytometry **39** (4), 285-294 (2000).

[2] D. Y. Jin, J. A. Piper, R. C. Leif et al., "Time-gated flow cytometry: an ultra-high selectivity method to recover ultra-rare-event mu-targets in high-background biosamples," Journal of Biomedical Optics **14** (2) (2009).

[3] N. Weibel, L. J. Charbonniere, M. Guardigli et al., "Engineering of highly luminescent lanthanide tags suitable for protein labeling and time-resolved luminescence imaging," Journal of the American Chemical Society **126** (15), 4888-4896 (2004).

[4] RC Leif, S. P. Clay, H. G. Gratzner et al., "Markers for Instrumental Evaluation of Cells of the Female Reproductive Tract: Existing and New Markers," presented at the The Automation of Uterine Cancer Cytology, Chicago, 1976 (unpublished).

[5] H. Siitari, I. Hemmila, E. Soini et al., "Detection of Hepatitis-B Surface-Antigen Using Time-Resolved Fluoroimmunoassay," Nature **301** (5897), 258-260 (1983); A. E. Soini and T. Lovgren, "Time-resolved fluorescence of lanthanide probes and applications in biotechnoloy," CRC CRITICAL REVIEWS IN ANALYTICAL CHEMISTRY **18**, 105-154 (1987).

[6] J. L. Yuan and G. L. Wang, "Lanthanide-based luminescence probes and time-resolved luminescence bioassays," Trac-Trends in Analytical Chemistry **25** (5), 490-500 (2006).

[7] J. C. G. Bunzli, "Lanthanide Luminescent Bioprobes (LLBs)," Chemistry Letters **38** (2), 104-109 (2009).

[8] P. R. Selvin, "Principles and biophysical applications of lanthanide-based probes," Annual Review of Biophysics and Biomolecular Structure **31**, 275-302 (2002).

[9] A. E. Soini, A. Kuusisto, N. J. Meltola et al., "A new technique for multiparameter imaging microscopy: Use of long decay time photoluminescent labels enables multiple color immunocytochemistry with low channel-to-channel crosstalk," Microscopy Research and Technique **62** (5), 396-407 (2003).

[10] S. Petoud, S. M. Cohen, J. C. G. Bunzli et al., "Stable lanthanide luminescence agents highly emissive in aqueous solution: Multidentate 2-hydroxyisophthalamide complexes of SM3+, Eu3+, Tb3+, Dy3+," Journal of the American Chemical Society **125** (44), 13324-13325 (2003).

[11] E. Deiters, B. Song, A. S. Chauvin et al., "Luminescent Bimetallic Lanthanide Bioprobes for Cellular Imaging with Excitation in the Visible-Light Range," Chemistry-a European Journal **15** (4), 885-900 (2009).

[12] A. Thibon and V. C. Pierre, "Principles of responsive lanthanide-based luminescent probes for cellular imaging," Analytical and Bioanalytical Chemistry **394** (1), 107-120 (2009); A. Thibon and V. C. Pierre, "A Highly Selective Luminescent Sensor for the Time-Gated Detection of Potassium," Journal of the American Chemical Society **131** (2), 434-+ (2009).

[13] S. B. D. Makhluf, R. Arnon, C. R. Patra et al., "Labeling of sperm cells via the spontaneous penetration of Eu3+ ions as nanoparticles complexed with PVA or PVP," Journal of Physical Chemistry C **112** (33), 12801-12807 (2008).

[14] J. Wu, Z. Q. Ye, G. L. Wang et al., "Visible-light-sensitized highly luminescent europium nanoparticles: preparation and application for time-gated luminescence bioimaging," Journal of Materials Chemistry **19** (9), 1258-1264 (2009).

[15] J. Wu, G. L. Wang, D. Y. Jin et al., "Luminescent europium nanoparticles with a wide excitation range from UV to visible light for biolabeling and time-gated luminescence bioimaging," Chemical Communications (3), 365-367 (2008).

[16] C. H. Song, Z. Q. Ye, G. L. Wang et al., "Preparation and time-gated luminescence bioimaging application of ruthenium complex covalently bound silica nanoparticles," Talanta **79** (1), 103-108 (2009).

[17] D. Y. Jin, R. Connally, and J. Piper, "Practical time-gated luminescence flow cytometry. I: Concepts," Cytometry Part A **71A**, 783-796 (2007).

[18] R. Connally and J. Piper, "Solid-state time-gated luminescence microscope with ultraviolet light-emitting diode excitation and electron-multiplying charge-coupled device detection," Journal of Biomedical Optics **13** (3) (2008).

[19] H. Harma, T. Soukka, and T. Lovgren, "Europium nanoparticles and time-resolved fluorescence for ultrasensitive detection of prostate-specific antigen," Clinical Chemistry **47** (3), 561-568 (2001).

[20] G. Vereb, E. Jares-Erijman, P. R. Selvin et al., "Temporally and spectrally resolved imaging microscopy of lanthanide chelates," Biophysical Journal **74** (5), 2210-2222 (1998).

[21] G. Yao, L. Wang, Y. R. Wu et al., "FloDots: luminescent nanoparticles," Analytical and Bioanalytical Chemistry **385** (3), 518-524 (2006).

[22] R. Connally, D. Y. Jin, and J. Piper, "High intensity solid-state UV source for time-gated luminescence microscopy," Cytometry Part A **69A** (9), 1020-1027 (2006).

[23] R. E. Connally and J. A. Piper, "Time-gated luminescence microscopy," Fluorescence Methods and Applications: Spectroscopy, Imaging, and Probes **1130**, 106-116 (2008).

[24] H. Kimura, M. Mukaida, M. Watanabe et al., "Quantitative evaluation of time-resolved fluorescence microscopy using a new europium label: Application to immunofluorescence imaging of nitrotyrosine in kidneys," Analytical Biochemistry **372** (1), 119-121 (2008); K. Hanaoka, K. Kikuchi, S. Kobayashi et al., "Time-resolved long-lived luminescence imaging method employing luminescent lanthanide probes with a new microscopy system," Journal of the American Chemical Society **129** (44), 13502-13509 (2007).

[25] D. Jin, R. Connally, and J. Piper, "Long-lived visible luminescence of UV LEDs and impact on LED excited time-resolved fluorescence applications," Journal of Physics D-Applied Physics **39** (3), 461-465 (2006).

[26] R. E. Connally and J. A. Piper, "Time-gated luminescence microscopy," in *Fluorescence Methods and Applications: Spectroscopy, Imaging, and Probes* (2008), Vol. 1130, pp. 106-116.

[27] R. C. Leif and S. Yang, "An analog method to produce time-gated images PW10B-BO127 (2010). {Publisher, please correct this reference.}."

[28] S. W. Botchway, M. Charnley, J. W. Haycock et al., "Time-resolved and two-photon emission imaging microscopy of live cells with inert platinum complexes," Proceedings of the National Academy of Sciences of the United States of America **105** (42), 16071-16076 (2008).

[29] D. J. Bornhop, D. S. Hubbard, M. P. Houlne et al., "Fluorescent tissue site-selective lanthanide chelate, Tb-PCTMB for enhanced imaging of cancer," Analytical Chemistry **71** (14), 2607-2615 (1999).

[30] A. Beeby, S. W. Botchway, I. M. Clarkson et al., "Luminescence imaging microscopy and lifetime mapping using kinetically stable lanthanide(III) complexes," Journal of Photochemistry and Photobiology B-Biology **57** (2-3), 83-89 (2000).